SCIENCE CHINA
Earth Sciences

• RESEARCH PAPER •

June 2010 Vol.53 No.6: 797–809
doi: 10.1007/s11430-010-3084-2

Eclogite-melt/peridotite reaction: Experimental constrains on the destruction mechanism of the North China Craton

WANG Chao[1,2*], JIN ZhenMin[1], GAO Shan[1], ZHANG JunFeng[1] & ZHENG Shu[1]

[1] *State Key Laboratory of Geological Processes and Mineral Resources, China University of Geosciences, Wuhan 430074, China;*
[2] *State Key Laboratory of Inorganic Synthesis and Preparative Chemistry, College of Chemistry, Jilin University, Changchun 130012, China*

Received October 26, 2009; accepted April 26, 2010

To study the mechanism of melt-peridotite reaction pertinent to the destruction of the North China Craton (NCC) lithosphere, a series of experiments were performed at a pressure of 2.0 GPa and temperatures from 1250 to 1400°C using Bixiling eclogite and Damaping peridotite as starting materials. The experimental results show that the reaction between eclogite melt and peridotite causes dissolution of olivine and orthopyroxene and precipitation of clinopyroxene in the melt. The experimental run products, characterized by a lherzolite/pyroxenite/garnet-pyroxenite sequence, are consistent with the mantle xenoliths in the Neogene Hannuoba basalt of the NCC found by Liu et al. (2005). It suggests that the mafic lower continental crust was probably recycled into the mantle during the Mesozoic Era. In the experiments conducted at 1300 and 1350°C, the resulting melts have a high Mg# andesite signature, indicating that the melt-peridotite reaction may have played a major role in the generation of high Mg# andesite. Our experimental results support the hypothesis that melts derived from foundered eclogite in the asthenosphere will consume the lithospheric peridotites. Therefore, melt-peridotite reaction is an important mechanism for the destruction/thinning of the lithosphere.

eclogite, peridotite, melt/peridotite reaction, high Mg# andesite, delamination, destruction of lithosphere

Citation: Wang C, Jin Z M, Gao S, et al. Eclogite-melt/peridotite reaction: Experimental constrains on the destruction mechanism of the North China Craton. Sci China Earth Sci, 2010, 53: 797–809, doi: 10.1007/s11430-010-3084-2

It is generally accepted that the North China Craton (NCC) lithosphere has lost ~150 km of thickness since the Paleozoic [1–4]. However, many aspects about the dynamics of this process are still under debated, especially the thinning mechanism. Two popular thinning mechanisms were proposed for NCC, one is the delamination model [5–7], and the other is thermo-mechanical and chemical erosion model [8–11]. Overall, the former is more suitable for interpreting the thinning of continental lithosphere, especially of thick lithosphere under an orogenic belt [12–14]. It has aroused great interest because of the investigation of Xilonggou high Mg# andesite [7], which was believed to originate as a result of a strontium rich and yttrium depleted melt derived from the foundered lower crustal eclogite with subsequent interaction with mantle peridotite. The discovery of zoned mantle olivine and pyroxene xenocrysts, and zoned mantle peridotitic xenoliths in the Mesozoic basaltic rocks from eastern North China by Yan et al. [15] and Zhang et al. [16–21], indicates that melt-peridotite reaction was widespread in Mesozoic lithospheric mantle beneath the southeastern NCC. Such interaction could be an important mechanism for the compositional transformation and rapid refertilization of the lithospheric mantle [16–18, 22–23]. However, Zhang et al. [24] proposed that the reaction between melt from foundered lower crust and mantle peridotite may not be the only way to generate the high Mg# andesites of western Liaoning. At least, two other processes

*Corresponding author (email: wangchao@cug.edu.cn)

© Science China Press and Springer-Verlag Berlin Heidelberg 2010

can also lead to the same result: (1) If there exists abundant olivine xenocrysts in the primary magma, interaction between them will increase the Mg# of the magma. In the subsequent stages of magma evolution, crystallization of olivine phenocrysts will then result in the decrease of MgO content. Undoubtedly, this absorption of high-Mg olivine and reprecipitation of low-Mg olivine process will increase the Mg# of the magma. (2) Mixing between primary basaltic magma and rhyolitic magma can also give rise to the formation of high Mg# andesite. Additionally, Xiong et al. [25] interpreted the strontium rich and yttrium depleted adakites as a result of the interaction between slab-derived melt and mantle peridotite.

The published high-pressure and high-temperature (HPHT) experimental investigations on the interaction between basalt and mantle-peridotite suggest two types of melt-peridotite reaction [26–28]. The first one is dissolution of olivine and clinopyroxene and precipitation of orthopyroxene, which will result in the formation of Si, Ca and Fe rich, but Mg poor melt. The other one is dissolution of orthopyroxene and precipitation of olivine and clinopyroxene, which will result in the formation of Si, Ca and Fe depleted, but Mg enriched melt. Based on cratonic mantle compositions worldwide, the correlation between Ni content in olivine and modal orthopyroxene of peridotites, and olivine volume changes during the reaction and porous flow features, Kelemen et al. [29] proposed that the first reaction tends to occur at shallow depths, which is thus unlikely to be widespread in the lithospheric mantle and thus the second reaction should be the major mode of melt-peridotite reaction in the lithospheric mantle. Experimental studies of Rapp et al. [30] indicate that reaction between silicic slab-derived melts and mantle peridotite can produce high Mg# adakitic melt and high Mg# andesite. All these studies mainly focused on the interaction between subducted oceanic slab melts and peridotite, which is different from NCC in terms of tectonic environment and geological characteristics. For instance, subducted oceanic crust contains a large quantity of water, while the lower crustal eclogites from NCC are essentially anhydrous. Up to now, there have been no anhydrous HPHT experimental investigations pertinent to the destruction mechanism of NCC. This has restricted further understanding of the dynamic mechanism for the thinning processes. All the knowledge about the lithospheric recycling of NCC is based on geochemical and geophysical studies and experiments on the interaction between subducted oceanic slab melts and peridotite.

Previous investigations showed that melt-peridotite reaction may be common in the Mesozoic and Cenozoic lithosphere mantle of NCC, which should be responsible for the compositional transformation and rapid fertilization of the lithospheric mantle. In light of the HPHT experiments, following questions need to be resolved to understand the relationship between melt-peridotite reaction and the thinning and replacement of NCC lithosphere: (1) What is the reaction mechanism of peridotite and melt with different compositions from different sources; (2) What is the relationship between the compositional characteristics of the reaction products and Mesozoic and Cenozoic lithosphere; (3) Can reaction between melts of foundered lower crust and mantle peridotite produce the high Mg# andesites of western Liaoning, and how in this reaction are the mineral assemblage and property of the melts changed; (4) Can the interaction of melts of subducted or foundered continental middle-lower crust with mantle peridotite result in rapid enrichment of the Mesozoic and Cenozoic NCC lithospheric mantle; and (5) How did the reaction between mantle derived basaltic melt and mantle peridotite contribute to the formation of the Cenozoic lithospheric mantle of oceanic affinities beneath NCC?

In this study, a series of HPHT experiments were conducted, using Bixiling eclogite and Damaping peridotite as starting materials, to reveal the reaction conditions and the compositional characters of eclogite-melt/peridotite reaction, which will constrain the delamination model and the mechanism of melt-peridotite reaction.

1 Experiments

1.1 Starting materials

Eclogite collected from Bixiling (Dabie Mountains) and a peridotite xenolith collected from Damaping (Hannuoba) were used as staring materials. The mineral assemblage of the eclogite is garnet + omphacite + quartz + accessory rutile. The mineral assemblage of the peridotite is olivine + orthopyroxene + clinopyroxene + spinel. Compositions of starting materials are given in Table 1. In order to avoid the grain size effect and uncertainty of natural samples, fresh samples of eclogite and peridotite were crushed and their minerals were separated. These were ground in an agate mortar for several hours to a grain size less than 5 μm. A mixture of these separates was prepared as staring materials. For all eclogite-melt/peridotite reaction experiments, eclogite and peridotite were combined in a two-layer geometric configuration, in which the upper-layer was peridotite and the bottom-layer was eclogite.

1.2 Experiment conditions

Because the experiments reported here were designed to simulate melts of foundered lower crust with subsequent interaction of the melts with mantle peridotite, a pressure equivalent to ~70 km depth of the lithosphere was selected as the experimental pressure. The temperature was selected according to the melting relationship of dry eclogite and peridotite determined by Anderson [31] (Figure 1). The solidus of anhydrous eclogite and peridotite are about 1150–1200 and 1400°C, respectively. Therefore, 1250–1400°C was chosen as the experimental temperature (Table 2). If the temperature is lower than 1250°C, the melt frac-

Table 1 Chemical compositions of whole rock and primary minerals of starting materials (wt%)[a)]

Oxide	Damaping lherzolite (DMP-018)					Bixiling eclogite (D95-25)			
	WR	Opx	Sp	Ol	Cpx	WR	Grt	Omp	Qz
SiO_2	44.31	56.26	0.03	41.09	52.98	48.08	39.51	55.86	99.42
TiO_2	0.07	0.11	0.09	0.03	0.51	0.75	0.04	0.05	0.032
Al_2O_3	2.28	3.79	57.01	0.03	6.15	19.31	22.80	10.59	0.039
Cr_2O_3	–	0.32	11.43	0.01	0.84	–	0.03	0.01	–
FeO	–	6.38	11.02	9.92	2.43	0.9	13.32	1.74	0.138
Fe_2O_3	8.66	–	–	–	–	8.32	–	–	0.027
MnO	0.12	0.14	0.12	0.14	0.08	0.15	0.33	0.01	0.015
MgO	42.71	32.26	20.03	48.29	14.18	8.53	9.03	10.03	0.018
CaO	1.68	0.44	0.01	0.02	20.75	10.84	14.13	14.70	0.016
Na_2O	0.26	0.06	0.02	0.01	1.87	2.03	0.02	6.07	–
K_2O	<0.01	0.00	0.00	0.01	0.01	0.05	–	–	–
P_2O_5	0.01	0.00	0.00	0.00	0.00	0.08	–	–	–
H_2O	–	–	–	–	–	0.68	–	–	–
NiO	–	–	–	–	–	–	0.01	0.02	–
Total	99.85	99.75	99.77	99.55	99.80	99.72	99.22	99.17	99.714

a) Initial eclogite proportions: 52 wt% garnet + 38 wt% omphacite + 10 wt% quartz + accessory rutile; initial lherzolite proportions: 66 wt% olivine+ 24 wt% orthopyroxene + 8 wt% clinopyroxene + 2 wt% spinel. The shown electron micro-probe analyses of component minerals from eclogites and peridotites were averaged over 5 or 6 measurements. WR, whole rock; Ol, olivine; Opx, orthopyroxene; Cpx, clinopyroxene, Sp, spinel; Grt, garnet; Omp, omphacite; Qz, quattz.; the same below.

Table 2 Experiment conditions and mineral assemblages of reaction products[a)]

Run No.	Experiment conditions				Starting materials	Mineral assemblages and percentage of reaction products	
	Pressure (GPa)	Temperature (°C)	Calculated temperature (°C)	Duration (h)			
012	2.0	1250	1235*, 1245**	72	Eclogite		Melt (7) + Cpx (37) + Grt (47) + Qz (2) + Pla (7)
015	2.0	1250		72	Eclogite + Peridotite	Peridotite zone	Ol + Opx + Cpx + Sp
						Garnet-pyroxenite zone	Melt (10) + Cpx (37) + Grt (47) + Qz (1) + Pla (5)
						Reaction zone	Cpx + Opx + Ol
017	2.0	1300	1302*, 1324**	72	Eclogite		Melt (27) + Cpx (38) + Grt (35)
018	2.0	1300		72	Eclogite + Peridotite	Peridotite zone	Ol + Opx + Cpx + Sp
						Garnet-pyroxenite zone	Melt (20) + Cpx (48) + Grt (32)
						Reaction zone	Cpx + Opx + Ol
021	2.0	1350	1332*, 1347**	48	Eclogite		Melt (60) + Cpx (22) + Grt (8)
					Eclogite + Peridotite	Peridotite zone	Ol + Opx + Cpx + Sp
						Garnet-pyroxenite zone	Melt (8) + Cpx (54) + Grt (38)
						Reaction zone	Cpx + Opx + Ol
023	2.0	1400		24	Eclogite		Melt (85) + Cpx (13) + Grt (2)
					Eclogite + Peridotite	Peridotite zone	Ol + Opx + Cpx + Sp
						Garnet-pyroxenite zone	Melt + Cpx +Grt
						Reaction zone	Cpx + Opx +Ol

a) Pla, plagioclase. The calculated temperature was calculated from the composition of coexisting garnet and clinopyroxene and the geothermometer of Ravna * [32], Ellis and Green** [33].

tion in eclogite-melt/peridotite reaction is too small to identify its chemical composition.

1.3 Experimental techniques

The experiments were conducted in a non-end-loaded type piston-cylinder (Quickpress 3.0) apparatus at the State key Laboratory of Geological Processes and Mineral Resources of China University of Geosciences. As shown in Figure 2, the assembly consists of a platinum (Pt) capsule sandwiched between two hexagonal Boron Nitride (h-BN) rods, in a graphite, Pyrex and salt sleeve. The Pt capsule was separated by a short h-BN sleeve from the graphite heater. The starting materials were encapsulated in a graphite tube (1 mm internal diameter, 2.8 mm outside diameter), which was subsequently placed in a Pt capsule (2.8 mm internal

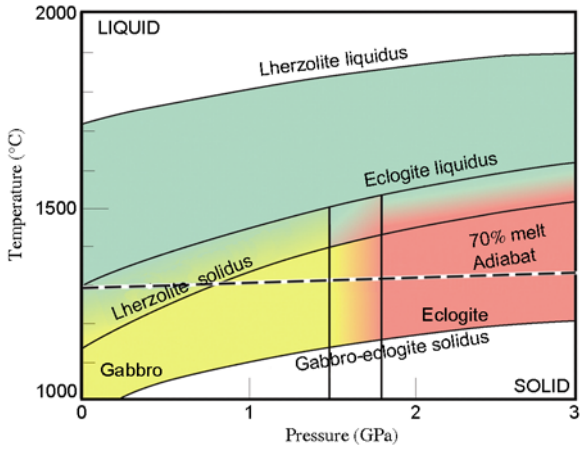

Figure 1 Melting relations in dry lherzolite and eclogite. The dashed line is a reference 1300°C mantle adiabat. The two vertical lines separate the gabbro field from the eclogite field (in between is the mixed phase region) [32].

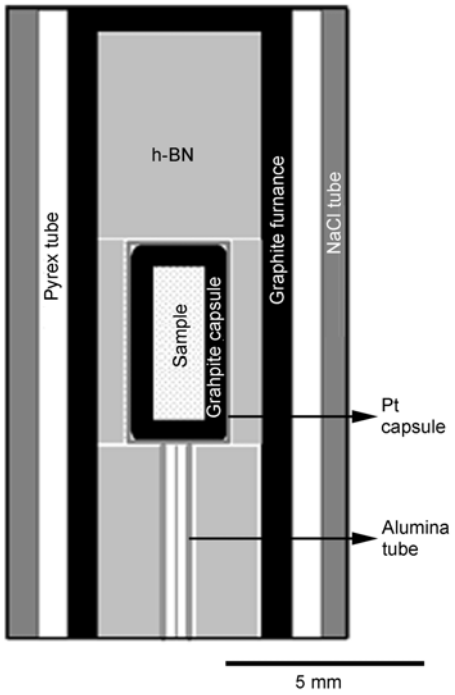

Figure 2 Piston-cylinder assembly.

diameter, 3.0 mm outside diameter). Prior to final sealing of the Pt tube, the open capsules were heated to 400°C in a muffle furnace for a minimum of 12 hours, in order to remove completely any water absorbed by the sample and the graphite capsule. The experimental temperature was monitored by inserting a W5Re-W26Re thermocouple into the high-pressure cell. For these experiments, temperature and pressure errors are expected to be less than 10°C and 0.1 GPa, respectively, based on previous calibration experiments in our laboratory (unpublished). Experiments were initially pressurized to 1.8 GPa with an increase rate of 10 MPa/min, and then were slowly heated to 1100°C. After standing half an hour to soften Pyrex, the pressure was increased first to 2 GPa before the target temperature was reached. Experiments were ended by turning off the power to the press, resulting in quenching to below 200°C within 10 s before the pressure was released. A quarter of the recovered Pt capsule was cut perpendicular to the cylindrical axis using a low-speed diamond saw. The remaining part was mounted in epoxy and polished to expose the sample (Figure 3). In all runs the graphite capsules appeared to have remained intact during the experiments, which effectively prevented contact of the sample with the outer Pt capsule.

1.4 Analyses of chemical composition

Whole rock major elements were analyzed by X-ray fluorescence spectrometry (Rikagu RIX 2100) at the State Key Laboratory of Continental Dynamics, Northwest University, China. The minerals of the starting materials and the experiment results were analyzed for major elements using a JEOL-JXA-8100 electron microprobe at China University of Geosciences. The accelerating voltage, beam current and counting time were set to 15 kV, 20 nA and 10 s, respectively. A focused beam (1 μm) was used for all mineral analyses to avoid overlap with mineral inclusions or quench overgrowths on grain rims. For melt analysis, the content of Na and K were firstly analyzed using a defocused beam (5–25 μm) to decrease their loss, where sufficiently large quenched glass pools were formed. Analyses conducted

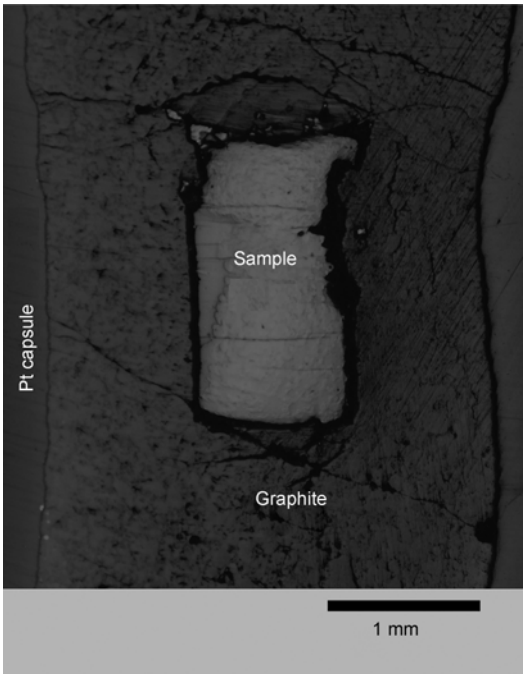

Figure 3 Photomicrograph of experimental charge of Run 017 (2.0 GPa, 1300ºC).

using a beam size larger than 10 μm resulted in melt compositions with major-element totals of between 97% and 100%.

2 Results

2.1 Partial melting of eclogite

Within error, no systematic variations in mineral compositions were found across the width or length of the experimental charges, apart form a few garnets with compositional zonation. Because the relative mass of these garnet cores is very small, the run products can be regarded approximately as an equilibrium system. Temperatures calculated from coexisting garnet-clinopyroxene pairs using geothermometers [32, 33] are within ±25°C for all experiments (Table 2), which also indicate equilibrium. Only analyses of garnets without zonation were used to calculate average compositions. Abundances of melt, clinopyroxene and garnet, were obtained by point counting, and are listed in Table 2. Their chemical compositions are shown in Table 3.

At 1250°C, the mineral assemblage of the run product consists of melt (7%) + clinopyroxene (37%) + garnet (47%) + feldspar (7%). A previous study of Pertermann and Hirschmann [34] has shown that the quartz should disappear between 1185–1225°C, which is different from our experiment. It is well known that melting point of quartz is far above 1250°C at 2 GPa. Therefore, the melting temperature of quartz in eclogite partial melting experiments depended on its saturation in the coexisting melt. Presence of quartz in the melt indicates that it is supersaturated at 1250°C. Quartz and feldspar are absent at 1300 and 1350°C, where the experimental product is comprised of melt, clinopyroxene and garnet. Although only melt and clinopyroxene were found in the backscattered electron images, there should be about 2% residual garnet at 1400°C, based on mass balance calculation. This indicates that the liquidus of dry eclogite exceeds 1400°C.

On a TAS diagram (Figure 4), melts from partial melting experiments are plotted in the fields of dacite, basaltic andesite and basalt. The correlations between composition of all minerals in experimental products and temperatures are shown in Figure 5. The content of SiO_2, TiO_2, Na_2O and K_2O of melt decreased with increasing temperature, while the content of Al_2O_3, FeO, MgO and CaO increased, which is in accordance with previous investigations [34, 35].

For all experiments, the ratio of Na/(Na+Ca) in the residual clinopyroxene is lower than 0.2, which means that most Na of the starting materials was dissolved into the melt. The Mg# and MgO contents of residual clinopyroxene increased with increasing temperature, where the Mg# increased from 74.5 at 1250°C to 81.4 at 1400°C. SiO_2, FeO, Al_2O_3 and CaO all have no obvious changes with temperature.

SiO_2, Al_2O_3 and MgO of residual garnet gradually increased with temperature, while FeO and CaO decreased, which indicated that the pyrope component in residual garnet has a positive correlation with temperature, and almandine and essonite have a negative correlation with tempera-

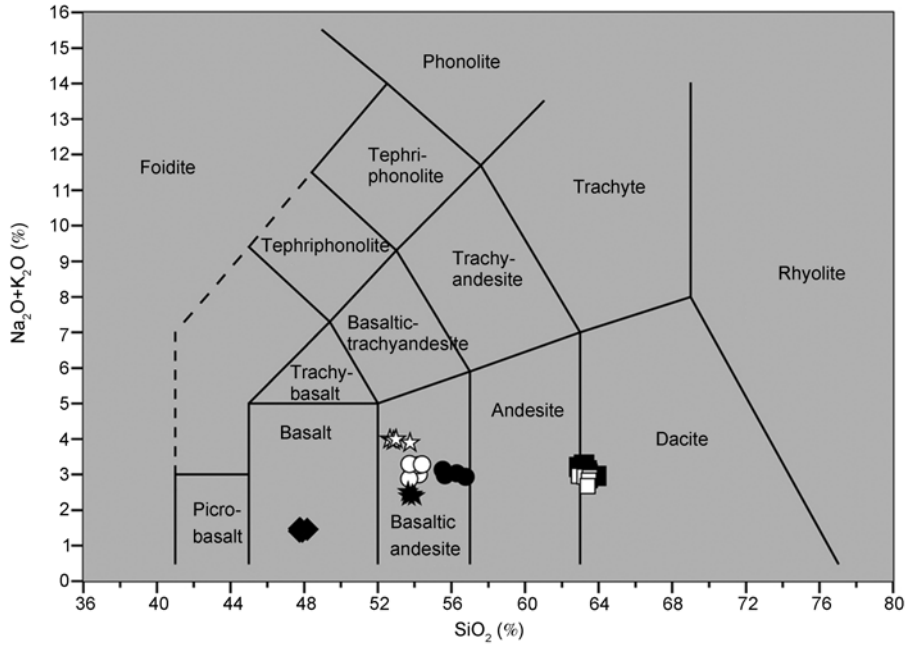

Figure 4 The SiO_2-(K_2O+Na_2O) diagram (TAS diagram) of melt compositions from the eclogite partial melting experiments and the eclogite-melt/peridotite reaction experiments. ■, ●, ★ and ◆ represent melts from eclogite partial melting experiments at 1250, 1300, 1350 and 1400°C, respectively; □, ○ and ☆ represent melts from eclogite-melt/peridotite reaction experiments, respectively.

Table 3 Chemical compositions (wt%) of eclogite-melt/peridotite reaction samples, conducted at 2 GPa, 1250–1400°C [a)]

	SiO_2	TiO_2	Al_2O_3	Cr_2O_3	FeO	MnO	MgO	CaO	Na_2O	K_2O	NiO	Total	Mg#
Partial melting of eclogite (1250°C)													
Melt	63.36	1.23	17.12	0.00	4.98	0.06	1.74	8.15	2.78	0.34	0.04	99.79	38.6
Cpx	48.33	0.99	13.97	0.05	6.03	0.07	9.79	18.53	1.78	–	0.04	99.58	74.5
Grt	39.65	0.16	22.44	0.04	14.64	0.30	9.19	13.03	0.02	–	0.05	99.52	53.0
Pla	57.45	0.05	26.11	0.00	0.44	0.00	0.08	9.52	5.80	0.09	0.03	99.58	
Eclogite-melt/peridotite reaction (1250°C)													
Reaction zone													
Opx-Zone	54.46	0.22	3.99	0.09	7.39	0.11	31.96	1.38	0.06	0.02	0.17	99.86	88.6
Cpx	50.16	0.27	11.30	0.06	5.74	0.10	12.23	17.88	1.73	–	0.07	99.53	79.3
Garnet-pyroxenite zone													
Melt1	62.94	0.73	17.49	0.00	5.06	0.05	2.09	8.48	2.77	0.18	0.06	99.84	42.7
Melt2	63.23	0.75	17.29	0.00	5.07	0.05	2.06	8.41	2.73	0.21	0.05	99.85	42.3
Melt3	63.53	0.73	17.26	0.01	4.99	0.06	1.98	8.54	2.64	0.21	0.04	99.97	41.6
Melt4	63.52	0.76	17.09	0.00	5.08	0.05	2.03	8.35	2.68	0.24	0.05	99.85	41.9
Melt5	63.48	0.78	17.33	0.00	5.04	0.05	1.95	8.22	2.66	0.17	0.00	99.69	41.1
Melt6	63.41	0.74	17.64	0.00	5.15	0.04	1.91	8.24	2.46	0.21	0.05	99.85	40.0
Cpx1	49.90	0.99	11.53	0.07	6.17	0.10	11.14	18.09	1.77	0.00	0.06	99.83	76.5
Cpx2	49.53	0.24	11.96	0.05	6.39	0.10	11.05	19.08	1.46	0.03	0.03	99.91	75.7
Cpx3	49.19	0.52	12.89	0.04	6.28	0.08	10.51	18.66	1.62	0.01	0.05	99.86	75.1
Cpx4	48.47	0.53	13.85	0.03	6.27	0.10	10.07	18.61	1.66	0.00	0.03	99.63	74.3
Cpx5	48.51	0.44	14.80	0.01	6.20	0.06	9.58	18.67	1.57	0.00	0.07	99.91	73.6
Grt1	39.53	0.28	22.33	0.03	15.45	0.34	10.57	10.46	0.05	0.01	0.03	99.09	55.2
Grt2	39.63	0.31	22.35	0.04	15.54	0.33	10.52	10.67	0.00	0.00	0.06	99.45	54.9
Grt3	39.53	0.28	22.33	0.03	15.45	0.34	10.57	10.46	0.05	0.01	0.03	99.09	55.2
Grt4	39.63	0.31	22.35	0.04	15.54	0.33	10.52	10.67	0.00	0.00	0.06	99.45	54.9
Grt5	39.55	0.07	22.59	0.02	15.42	0.28	10.17	11.27	0.02	0.00	0.04	99.44	54.3
Peridotite zone													
Ol1	39.45	0.02	0.10	0.01	11.60	0.10	47.58	0.18	0.00	0.00	0.44	99.48	88.10
Ol2	39.79	0.00	0.05	0.00	10.64	0.12	48.51	0.16	0.00	0.01	0.37	99.65	89.10
Ol3	39.63	0.02	0.08	0.02	10.86	0.10	48.14	0.15	0.01	0.01	0.42	99.97	88.9
Ol4	39.81	0.03	0.06	0.02	10.12	0.11	48.69	0.13	0.02	0.01	0.40	99.41	89.7
Ol5	40.10	0.02	0.07	0.02	9.18	0.14	49.63	0.12	0.01	–	0.38	99.68	90.7
Ol6	40.07	0.02	0.05	0.00	9.21	0.14	49.38	0.12	0.02	0.01	0.39	99.41	90.6
Opx1	55.47	0.10	3.23	0.03	6.52	0.12	33.00	1.11	0.05	0.00	0.16	99.78	90.1
Opx2	55.06	0.11	3.67	0.34	6.03	0.11	33.65	0.48	0.02	0.00	0.09	99.55	90.9
Opx3	55.27	0.11	3.49	0.30	5.96	0.12	33.84	0.40	0.04	–	0.12	99.66	91.1
Cpx1	51.71	0.45	6.23	0.93	3.29	0.06	16.87	18.69	1.72	–	0.11	99.55	90.2
Cpx2	53.47	0.44	5.27	0.90	2.90	0.05	16.05	21.16	1.34	0.00	0.08	101.66	90.9
Cpx3	53.78	0.43	5.34	0.87	2.94	0.07	15.49	20.87	1.58	0.00	0.12	101.48	90.5
Cpx4	53.29	0.46	5.65	0.92	2.97	0.04	15.78	20.53	1.35	0.01	0.10	101.10	90.5
Sp	0.10	0.19	52.96	13.45	13.50	0.08	19.42	0.10	0.00	0.02	0.39	100.22	
Partial melting of eclogite (1300°C)													
Melt	56.30	0.64	18.71	0.00	7.35	0.11	3.21	10.60	2.92	0.11	0.06	99.99	44.0
Cpx	48.02	0.39	13.95	0.05	6.18	0.08	10.90	18.76	1.41	0.01	–	99.75	76.1
Grt	40.10	0.30	22.51	0.02	13.67	0.40	12.71	10.09	0.02	0.00	0.00	99.85	62.6
Eclogite-melt/peridotite reaction (1300°C)													
Reaction zone													
Opx-zone	52.91	0.15	6.05	0.10	9.56	0.10	28.96	1.84	0.12	–	–	99.79	84.5
Cpx	50.47	0.21	9.75	0.13	7.53	0.13	15.95	14.49	1.11	–	–	99.78	79.2
Garnet-pyroxenite zone													
Melt1	54.01	0.70	16.45	0.00	9.44	0.11	6.59	8.94	3.06	0.12	0.00	99.43	55.70
Melt2	53.88	0.69	16.38	0.00	9.34	0.09	6.45	8.79	3.04	0.12	0.00	98.80	55.40
Melt3	54.24	0.71	16.38	0.00	9.37	0.08	6.33	8.82	2.87	0.13	0.00	98.92	54.90
Melt4	53.71	0.66	16.52	0.01	9.25	0.09	6.12	8.80	2.77	0.11	0.00	98.04	54.40

(*To be continued on the next page*)

(*Continued*)

	SiO_2	TiO_2	Al_2O_3	Cr_2O_3	FeO	MnO	MgO	CaO	Na_2O	K_2O	NiO	Total	Mg#
Melt5	54.23	0.69	16.79	0.00	9.24	0.10	5.42	8.95	3.12	0.14	0.00	98.67	51.40
Melt6	53.73	0.73	16.63	0.01	9.33	0.08	5.68	9.12	3.16	0.13	0.00	98.59	52.30
Melt7	54.41	0.73	16.83	0.02	9.23	0.10	5.06	8.69	3.14	0.13	0.00	98.34	49.7
Cpx1	49.74	0.24	11.39	0.09	6.72	0.12	14.12	16.29	1.13	0.01	0.00	99.84	79.1
Cpx2	48.75	0.24	12.71	0.03	6.29	0.09	12.17	18.40	1.22	0.00	0.00	99.89	77.7
Cpx3	49.18	0.22	12.11	0.09	6.54	0.11	13.25	17.17	1.11	0.00	0.00	99.78	78.5
Cpx4	47.26	0.28	14.99	0.07	6.14	0.10	11.19	18.39	1.25	0.01	0.00	99.70	76.6
Cpx5	46.60	0.28	16.19	0.05	6.14	0.11	10.36	18.95	1.14	0.02	0.00	99.85	75.2
Cpx6	45.79	0.28	17.17	0.04	6.21	0.05	9.88	19.17	1.20	0.00	0.00	99.79	74.1
Cpx7	46.79	0.27	15.79	0.02	6.23	0.11	10.29	19.10	1.10	0.01	0.00	99.69	74.8
Cpx8	47.34	0.28	15.15	0.03	6.18	0.12	10.70	18.90	1.17	0.00	0.00	99.88	75.7
Grt1	40.58	0.20	22.88	0.10	12.87	0.33	15.25	7.23	0.00	0.00	0.00	99.44	68.1
Grt2	40.81	0.20	22.93	0.12	12.64	0.33	15.91	6.85	0.01	0.00	0.00	99.81	69.4
Grt3	40.77	0.21	22.81	0.14	12.68	0.32	15.81	6.86	0.02	0.01	–	99.62	69.2
Grt4	40.66	0.24	22.71	0.07	13.13	0.31	14.97	7.39	0.00	0.00	0.00	99.49	67.2
Grt5	40.77	0.24	22.95	0.01	13.35	0.34	14.59	7.28	0.03	0.00	0.00	99.56	66.3
Peridotite zone													
Ol1	40.09	0.04	0.14	0.02	14.66	0.07	44.64	0.24	0.02	0.01	0.00	99.94	84.6
Ol2	40.21	0.04	0.14	0.03	13.70	0.10	45.50	0.23	0.02	0.01	–	99.97	85.7
Ol3	40.32	0.04	0.14	0.03	12.75	0.12	46.36	0.23	0.02	0.00	0.00	100.00	86.7
Ol4	40.93	0.04	0.12	0.04	10.01	0.09	48.33	0.23	0.04	0.00	0.00	99.80	89.7
Ol5	40.70	0.03	0.12	0.05	9.94	0.12	48.64	0.20	0.02	0.00	0.00	99.81	89.8
Ol6	40.74	0.04	0.12	0.06	9.62	0.11	48.98	0.20	0.02	0.00	–	99.89	90.2
Ol7	40.50	0.03	0.08	0.06	9.38	0.12	49.48	0.22	0.01	0.00	0.00	99.88	90.5
Ol8	40.55	0.06	0.11	0.02	9.68	0.10	49.00	0.22	0.02	0.00	0.00	99.77	90.1
Opx1	55.44	0.13	3.78	0.38	6.02	0.12	33.43	0.54	0.07	0.00	0.00	99.91	90.9
Opx2	55.41	0.08	3.47	0.31	6.05	0.12	34.04	0.41	0.01	0.03	0.00	99.91	91.0
Opx3	55.50	0.10	3.42	0.27	5.99	0.16	33.83	0.46	0.03	0.00	0.00	99.75	91.1
Opx4	55.61	0.10	3.30	0.27	6.02	0.13	34.00	0.41	0.02	0.01	–	99.88	91.0
Cpx1	51.49	0.67	7.36	0.71	3.77	0.08	18.55	15.56	0.99	0.00	0.00	99.18	89.9
Cpx2	51.98	0.43	5.66	0.85	2.90	0.07	15.55	20.72	1.30	0.00	0.00	99.45	90.6
Cpx3	52.77	0.40	5.50	0.67	3.90	0.07	20.98	14.31	0.87	–	–	99.48	90.6
Sp	0.21	0.20	52.87	15.24	8.10	0.11	21.94	0.01	0.03	0.00	0.44	99.12	
Partial melting of Eclogite (1350°C)													
Melt	53.68	0.52	18.82	0.00	8.82	0.14	5.07	9.91	2.32	0.06	0.00	99.34	50.9
Cpx	47.98	0.22	14.02	0.09	6.26	0.10	11.70	18.72	1.41	–	0.04	100.54	77.1
Grt	40.13	0.08	23.77	0.03	13.22	0.36	15.02	8.16	0.01	0.00	0.00	100.78	67.2
Eclogite-melt/peridotite reaction (1350°C)													
Reaction zone													
Opx-zone	51.82	0.23	7.07	0.15	8.80	0.13	29.34	1.97	0.11	0.00	0.19	99.80	85.7
Cpx1	51.34	0.44	9.83	0.15	5.82	0.05	18.00	12.90	1.07	0.00	0.09	99.7	84.80
Cpx2	50.93	0.33	9.64	0.07	6.32	0.10	17.77	13.60	1.02	0.00	0.18	99.77	83.5
Cpx3	51.14	0.38	9.74	0.11	6.07	0.08	17.88	13.25	1.04	0.00	0.13	99.73	84.10
Grt1	41.99	0.39	22.92	0.12	9.56	0.22	19.01	5.67	0.05	0.02	0.05	99.99	78.20
Grt2	41.46	0.24	23.53	0.12	9.97	0.22	18.66	5.39	0.01	0.01	0.04	99.65	77.10
Grt3	41.22	0.31	23.55	0.10	9.84	0.21	18.86	5.62	0.03	0.00	0.10	99.83	77.5
Garnet-pyroxenite zone													
Melt1	52.66	0.74	18.08	0.00	9.48	0.12	6.69	8.01	3.81	0.19	0.06	99.84	56.00
Melt2	52.85	0.74	17.64	0.00	9.45	0.12	6.49	8.01	3.82	0.13	0.05	99.31	55.30
Melt3	53.75	0.73	18.02	0.00	9.36	0.07	5.73	7.89	3.69	0.20	0.05	99.48	52.4
Melt4	52.99	0.78	18.21	0.00	9.52	0.11	5.01	7.69	3.78	0.20	0.03	98.33	48.7
Cpx4	49.32	0.16	10.23	0.11	5.89	0.09	14.56	15.76	1.33	0.00	0.07	97.52	81.6
Cpx5	48.10	0.25	13.53	0.03	6.28	0.11	12.39	18.15	1.32	0.00	0.08	100.25	78.0
Cpx6	48.21	0.30	13.08	0.09	6.33	0.11	12.62	17.84	1.23	0.01	0.04	99.86	78.2
Cpx6	48.13	0.26	13.36	0.07	6.30	0.10	12.42	18.10	1.30	0.01	0.07	100.09	78.0

(*To be continued on the next page*)

(*Continued*)

	SiO_2	TiO_2	Al_2O_3	Cr_2O_3	FeO	MnO	MgO	CaO	Na_2O	K_2O	NiO	Total	Mg#
Grt4	40.44	0.18	23.40	0.09	12.49	0.30	16.68	6.11	0.02	0.00	0.06	99.76	70.6
Grt5	40.85	0.20	23.36	0.07	12.79	0.29	16.59	6.01	0.01	0.00	0.01	100.19	70.0
Grt6	40.47	0.19	23.37	0.07	13.50	0.37	14.74	7.04	0.00	0.02	0.06	99.82	65.6
Grt7	40.44	0.22	23.00	0.08	13.63	0.35	15.32	6.97	0.01	0.00	0.03	100.03	66.9
Grt8	40.45	0.21	23.18	0.07	13.36	0.36	15.53	7.05	0.01	0.01	0.05	100.28	67.7
Peridotite zone													
Ol1	39.51	0.03	0.09	0.02	13.02	0.13	46.22	0.22	0.00	0.02	0.28	99.53	86.50
Ol2	39.44	0.04	0.08	0.03	12.33	0.11	46.92	0.16	0.01	0.00	0.42	99.54	87.3
Ol3	39.90	0.00	0.09	0.00	12.05	0.13	48.04	0.21	0.01	0.00	0.37	100.79	87.8
Ol4	39.66	0.02	0.13	0.04	11.85	0.13	47.81	0.24	0.00	0.00	0.39	100.26	87.90
Ol5	40.05	0.03	0.12	0.02	11.44	0.12	47.84	0.19	0.00	0.00	0.41	100.23	88.30
Ol6	40.56	0.02	0.13	0.04	10.00	0.11	48.90	0.21	0.03	0.00	0.40	100.39	89.80
Ol7	40.16	0.05	0.12	0.01	10.04	0.11	48.25	0.23	0.01	0.00	0.36	99.34	89.6
Opx1	52.31	0.23	6.21	0.27	7.84	0.13	29.68	1.90	0.13	0.00	0.19	98.89	87.2
Opx2	51.53	0.23	7.85	0.13	7.61	0.10	29.97	1.69	0.16	0.00	0.15	99.43	87.6
Opx3	53.21	0.16	4.78	0.29	7.71	0.13	31.18	1.32	0.15	0.01	0.15	99.07	87.9
Opx4	53.65	0.19	4.39	0.30	6.89	0.13	31.91	1.72	0.17	0.00	0.13	99.50	89.3
Opx5	54.62	0.13	3.47	0.34	6.87	0.06	32.85	0.89	0.11	0.00	0.18	99.52	89.6
Cpx7	48.25	0.35	6.70	0.43	6.21	0.11	22.44	12.73	0.83	0.00	0.13	98.2	86.7
Cpx8	49.25	0.35	6.70	0.43	4.61	0.11	21.44	14.73	0.83	0.00	0.13	98.59	89.3
Sp	0.08	0.26	54.60	13.53	10.57	0.11	20.00	0.02	0.00	0.00	0.36	99.52	
Partial melting of eclogite (1400°C)													
Melt	47.74	0.39	19.29	0.00	10.37	0.19	7.30	12.21	1.36	0.05	0.02	98.91	55.9
Cpx	47.26	0.18	14.31	0.12	5.38	0.16	13.11	18.47	0.64	0.00	0.03	99.65	81.4
Eclogite-melt/peridotite reaction (1400°C)													
Garnet-pyrxoenite zone													
Ol1	39.11	0.05	0.08	0.01	14.10	0.14	45.70	0.29	0.00	0.00	0.00	99.5	85.4
Opx1	52.19	0.13	8.44	0.23	8.84	0.12	27.52	2.20	0.17	0.00	0.00	99.80	84.9
Cpx1	51.76	0.15	7.09	0.72	6.25	0.11	21.72	11.21	0.66	0.00	0.00	99.67	86.2
Cpx2	51.01	0.22	8.44	0.18	6.04	0.12	19.51	13.54	0.74	0.00	0.00	99.79	85.3
Cpx3	50.97	0.18	8.97	0.15	6.37	0.13	19.65	12.77	0.69	0.00	0.00	99.86	84.7
Cpx4	50.23	0.16	8.25	0.10	6.29	0.14	19.37	13.36	0.71	0.00	0.00	98.61	84.7
Cpx5	51.13	0.15	8.30	0.16	6.52	0.15	20.27	12.09	0.74	0.00	0.00	99.51	84.8
Cpx6	51.49	0.14	7.40	0.10	5.91	0.12	19.49	14.01	0.80	0.01	0.00	99.47	85.6
Cpx7	50.97	0.18	8.97	0.15	6.37	0.13	19.65	12.77	0.69	0.00	0.0	99.9	84.7
Grt1	41.84	0.15	23.26	0.24	8.26	0.22	20.22	5.47	0.02	0.01	0.0	99.7	81.5
Grt2	41.82	0.15	23.23	0.22	8.41	0.19	20.34	5.35	0.00	0.00	0.0	99.7	81.3
Grt3	41.65	0.19	23.29	0.28	8.48	0.19	20.09	5.21	0.00	0.02	0.0	99.4	81
Grt4	41.70	0.21	23.03	0.29	8.45	0.24	20.29	5.27	0.00	0.01	0.0	99.5	81.2
Peridotite zone													
Ol2	39.37	0.03	0.11	0.00	13.86	0.16	45.94	0.25	0.03	0.00	0.00	99.73	85.6
Ol3	39.85	0.03	0.07	0.00	13.68	0.14	45.74	0.31	0.01	0.01	0.00	99.83	85.8
Ol4	39.51	0.03	0.11	0.02	13.51	0.12	46.28	0.29	0.00	0.00	0.00	99.87	86.0
Ol5	39.46	0.01	0.05	0.00	13.33	0.09	46.34	0.25	0.00	0.00	0.00	99.5	86.2
Ol6	39.17	0.00	0.11	0.01	13.72	0.11	46.32	0.28	0.01	0.01	0.00	99.74	85.9
Ol6	39.54	0.00	0.11	0.02	13.27	0.11	46.47	0.21	0.00	0.02	0.00	99.76	86.3
Ol7	39.83	0.02	0.10	0.02	12.03	0.11	47.29	0.22	0.00	0.00	0.00	99.616	87.6
Ol8	39.32	8.00	0.11	0.02	11.83	0.10	48.03	0.22	0.00	0.00	0.00	99.7	88.0
Ol9	39.92	0.02	0.11	0.02	11.43	0.10	48.12	0.20	0.00	0.00	0.00	99.93	88.3
Ol10	40.01	0.03	0.12	0.10	10.58	0.11	48.48	0.26	0.01	0.01	0.00	99.72	89.2
Ol11	39.88	0.02	0.14	0.09	9.62	0.09	49.31	0.24	0.04	0.01	0.00	99.43	90.2
Ol12	40.33	0.05	0.11	0.06	9.47	0.11	49.12	0.25	0.00	0.00	0.00	99.52	90.3
Ol13	40.49	0.03	0.18	0.06	9.42	0.10	48.85	0.27	0.00	0.03	0.00	99.44	90.3
Opx2	52.39	0.13	7.44	0.23	7.84	0.12	29.25	2.06	0.16	0.00	0.00	99.61	87.0
Opx3	52.36	0.21	8.01	0.28	6.81	0.10	29.44	2.09	0.18	0.00	0.00	99.49	88.6

(*To be continued on the next page*)

(*Continued*)

	SiO_2	TiO_2	Al_2O_3	Cr_2O_3	FeO	MnO	MgO	CaO	Na_2O	K_2O	NiO	Total	Mg#
Opx4	55.42	0.09	3.21	0.30	6.24	0.13	33.65	0.44	0.04	0.00	0.00	99.52	90.7
Opx5	55.31	0.11	3.50	0.30	6.16	0.11	33.40	0.52	0.04	0.00	0.00	99.44	90.7
Opx6	55.68	0.10	3.33	0.28	6.04	0.14	34.04	0.37	0.01	0.00	0.00	100.00	91.0
Cpx8	51.43	0.16	7.97	0.17	6.38	0.13	20.58	12.22	0.61	0.01	0.00	99.64	85.3
Cpx9	51.76	0.15	7.09	0.72	6.25	0.11	21.72	11.21	0.66	0.00	0.00	99.67	86.2
Cpx10	50.84	0.38	8.51	0.44	5.01	0.12	19.06	14.58	0.83	0.00	0.00	99.76	87.3
Cpx11	50.47	0.35	8.84	0.29	5.35	0.11	20.04	13.45	0.79	0.00	0.00	99.7	87.1
Cpx12	48.27	0.14	5.57	0.58	7.05	0.10	28.12	9.09	0.54	0.00	0.0	99.446	87.8
Cpx13	51.49	0.24	7.35	0.90	4.29	0.08	20.54	14.35	0.57	0.01	0.00	99.8	89.6
Cpx14	51.19	0.27	7.55	0.80	4.49	0.10	20.61	13.87	0.60	0.00	0.0	99.476	89.2
Sp	0.17	0.19	53.76	13.60	10.59	0.12	19.89	0.02	0.00	0.02	0.00	98.3	

a) All Fe was assumed to be Fe^{2+}; Mg# = Mg/(Mg+Fe^{2+}) × 100. The chemical composition of sample from eclogite partial melting experiment was the average of 5–7 measurements.

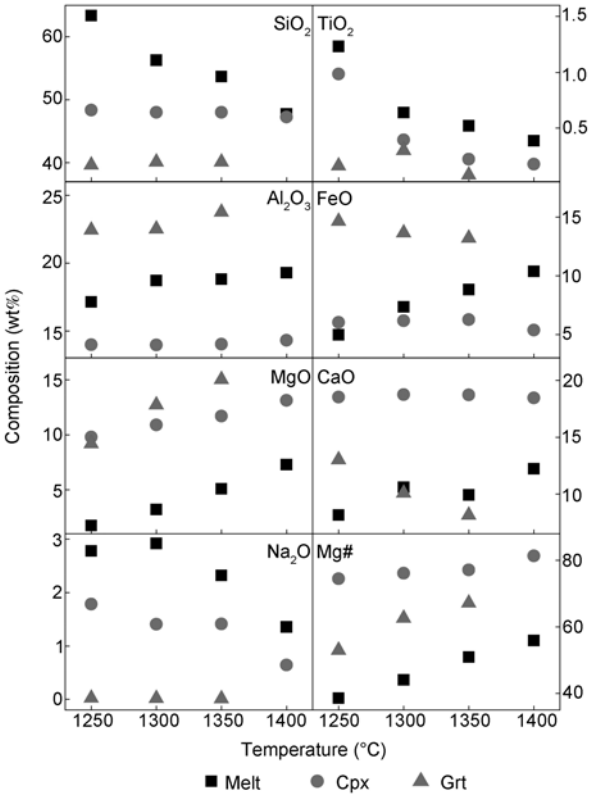

Figure 5 Composition of partial melts from eclogite partial melting experiments.

ture. Modal garnet decreased rapidly from 50% in starting material to 2% at 1400°C with increasing temperature.

2.2 Eclogite-melt/peridotite reaction

After the experiments, the samples contain three zones of melt including garnet-pyroxenite and partially hybridized peridotite separated by a reaction zone (Figure 6(a)–(c)). At 1400°C, the experimental product consists of a peridotite zone and a garnet-pyroxenite zone (Figure 6(d)), where eclogite melt was totally consumed.

(i) Reaction zone. The transition zone is comprised of two layers (Figure 6(a)–(c)): (1) a low Mg# (84.5–88.6) orthopyroxene-zone adjacent to the peridotite zone, which had a thickness of about 5–10 μm in all experiments; (2) a clinopyroxene layer which contains a small amount of garnet. The Mg# of clinopyroxene in layer 2 is higher than that in the garnet-pyroxenite zone, but lower than that in the peridotite zone (Figure 7(a)–(c)), which indicated that it is the result of eclogite-melt/peridotite reaction.

(ii) Peridotite zone. In addition to reaction with peridotite at the eclogite/peridotite interface, the eclogite melt also infiltrates into the peridotite zone along grain boundaries. The Mg# of olivine, orthopyroxene and clinopyroxene of peridotite decreased towards the low-Mg orthopyroxene zone/peridotite interface (Figure 7(a)–(d)), while CaO and FeO increased, which shows a typical diffusion characteristic. In summary, the eclogite-melt/peridotite reaction will result in evolution of peridotite towards a more Ca and Fe rich, but Mg depleted composition.

(iii) Garnet-pyroxenite zone. There is an obvious correlation of Mg# of melt, clinopyroxene and garnet in the garnet-pyroxenite zone with their distance from the eclogite/peridotite interface (Figure 7(a)–(d)). This indicates that the reaction did not reach equilibrium. However, it can be regarded approximately that the melt and minerals near the transition zone are in equilibrium. So their compositions were used in the following discussion of eclogite-melt/peridotite reaction.

At 1250°C, the garnet-pyroxenite zone consists of melt + clinopyroxene + garnet + feldspar + quartz. Quartz and feldspar disappear above 1300°C, which is similar to the result of eclogite partial melting experiments. The Mg# values of melts from experiments at the temperature from 1250 to 1350°C are 42.7, 55.7 and 56, respectively. On a TAS diagram (Figure 4), the melt from experiment at 1250°C plots in the andesite field, while the melts from experiments at 1300 and 1350°C plot in the basaltic andesite field, and are high-Mg# andesites (Mg# > 45). The composition changes of melt, clinopyroxene and garnet between partial melting and melt/peridotite reaction experiments are shown in Figure 8. It can be seen that garnet-melt/peridotite reaction increases Mg#, but decreases CaO of the melts,

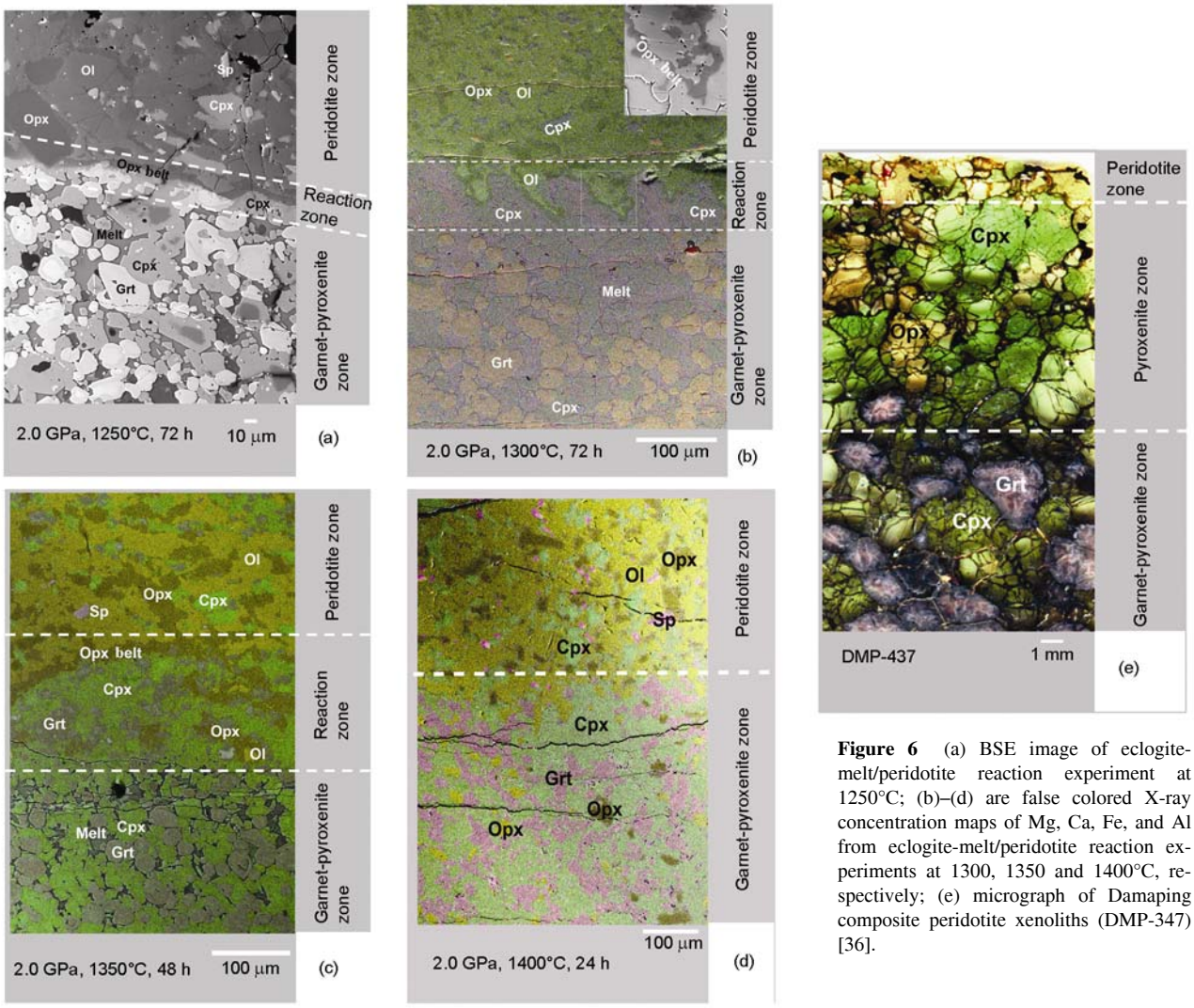

Figure 6 (a) BSE image of eclogite-melt/peridotite reaction experiment at 1250°C; (b)–(d) are false colored X-ray concentration maps of Mg, Ca, Fe, and Al from eclogite-melt/peridotite reaction experiments at 1300, 1350 and 1400°C, respectively; (e) micrograph of Damaping composite peridotite xenoliths (DMP-347) [36].

clinopyroxene and garnet. It should be noted that the proportion of melt in eclogite-melt/peridotite reaction experiment has greatly decreased relative to that in eclogite partial melting experiment, while the proportions of clinopyroxene and garnet have greatly increased, especially at temperatures above 1300°C. The result implies precipitation of abundant clinopyroxene and garnet from eclogite melt, along with melt/peridotite reaction and compositional change of melt.

3 Discussion

3.1 Mechanism of eclogite-melt/peridotite reaction

Because the starting materials are homogeneous, it is concluded from the micro-structures of the run products that the orthopyroxene zone and garnet bearing clinopyroxene layer are the result of eclogite-melt/peridotite reaction. Some investigations on the interaction between silicic melt and peridotite were already reported in the refs. [29, 37, 38]. However, all these studies came to the same conclusion that the reaction will consume olivine to produce orthopyroxene, which is different from the formation of clinopyroxene in our experiments. Orthopyroxene is Mg, Fe rich and Ca, Na depleted, compared to clinopyroxene. Therefore, formation of either clinopyroxene or orthopyroxene in eclogite-melt/peridotite reaction mainly depends on the CaO content of the melt. Omphacite will be rapidly converted to augite even with a low melt fraction, which dissolves a great amount of Na in the melt (Table 3). In addition, the CaO content of Bixiling eclogite is relatively high (Table 4). Therefore, we propose that the composition of eclogite, especially the CaO content, is a crucial factor for the formation of clinopyroxene or orthopyroxene in eclogite-melt/peridotite reaction (i.e. if the eclogite is Ca-rich, the result will be clinopyroxene, otherwise it will be orthopyroxene). However, the eclogite-melt/peridotite reaction is a complicated process. At the initial stage, consumption of olivine and orthopyroxene by eclogite-melt will generate clinopyroxene. With the reaction progressing, the CaO content of

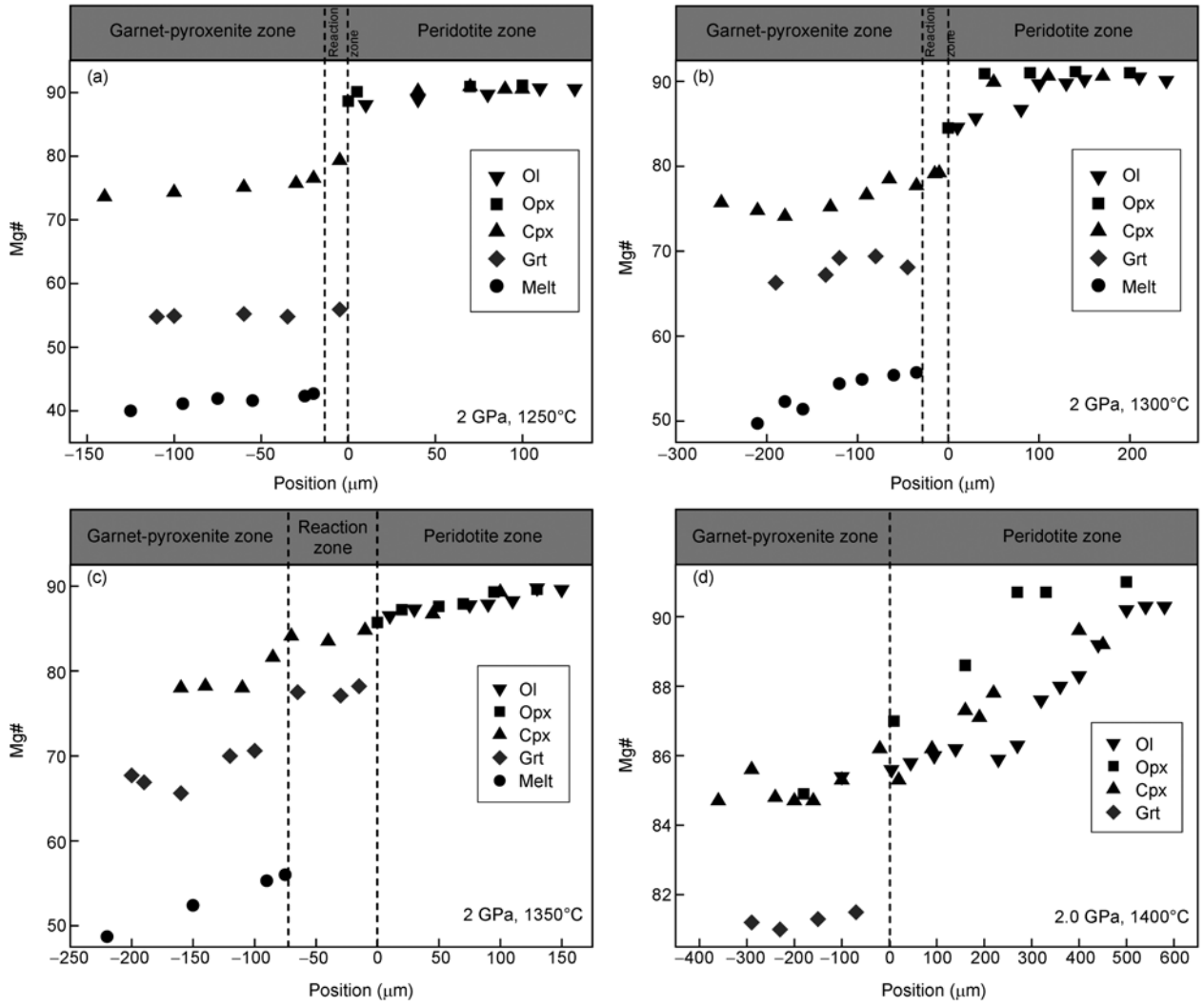

Figure 7 Plots of measured Mg# in olivine, orthopyroxene, clinopyroxene, garnet and melt as a function of distance in all eclogite-melt/peridotite reactions, the interface of low Mg# orthopyroxene-zone and peridotite is at $x = 0$ μm.

Table 4 Composition of basaltic starting materials used in this and other experimental studies (wt%)[a)]

Oxide	B95-25	AB-1	GA1	MONT147
SiO_2	48.08	51.19	50.35	54.86
TiO_2	0.75	1.18	1.49	0.77
Al_2O_3	19.31	16.62	16.53	18.78
Cr_2O_3	–	–	–	–
FeO	0.9	11.32	9.83	8.96
Fe_2O_3	8.32	–	–	–
MnO	0.15	0.23	0.17	0.21
MgO	8.53	6.59	7.94	3.66
CaO	10.84	5.49	9.60	8.80
Na_2O	2.03	4.33	3.49	3.08
K_2O	0.05	0.82	0.44	0.78
P_2O_5	0.08	–	0.16	0.14
H_2O	0.68	–	–	–
NiO	–	–	–	–
CaO/SiO_2	0.23	0.11	0.19	0.16
Total	99.72	99.30	100	100.02

a) B95-25, this study; Ab-1, Kelemen et al. [29]; GA1, Yaxley & Green [37]; MONT147, Morgan and Liang [38].

eclogite-melt will be greatly decreased to form a Si-rich and Ca-poor melt, which will react with olivine to form orthopyroxene and make an Mg-Ca exchange with the residual clinopyroxene and garnet to raise the CaO content of the coexisting melt. The increase of CaO concentration of melt will result in pre-existing orthopyroxene to be converted to clinopyroxene. Here we use four equilibrium steps to approximate the eclogite-melt/peridotite reaction [39]:

Step 1: Olivine + Melt1 → clinopyroxene + Melt2;

Step 2: Olivine + Melt2 → orthopyroxene + Melt3;

Step 3: Melt3 + residual Ca-rich clinopyroxene + garnet → Melt4 + Mg-rich and Ca-poor clinopyroxene + garnet (Ca-Mg exchange between residual clinopyroxene and Melt3);

Step 4: Melt4 + orthopyroxene → clinopyroxene + Melt5.

Melt1 can be regarded as the melt from eclogite partial melting. Melt5 can be regarded as the result of eclogite-

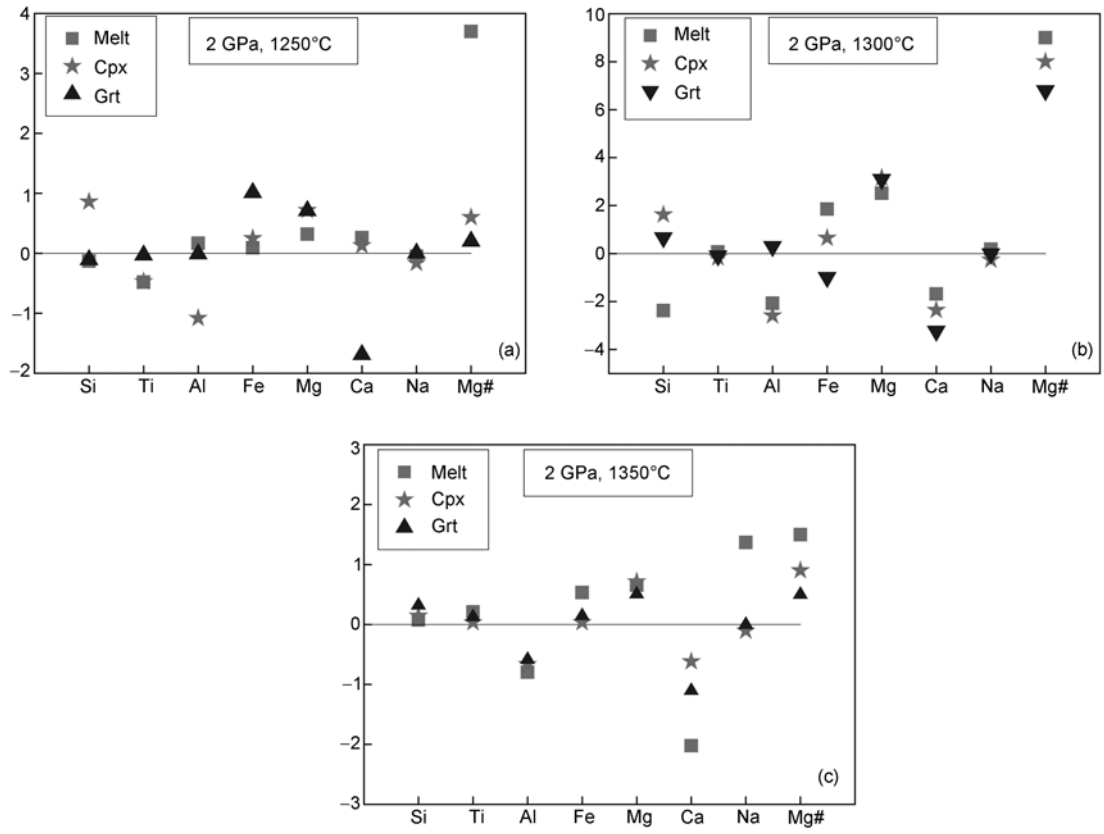

Figure 8 The composition differences between melt and component minerals from eclogite partial melting and eclogite-melt/peridotite reaction (garnet-pyroxenite zone). The *y*-coordinate is the difference of percent contents of oxides.

melt/peridotite reaction. The other three are intermediate virtual melts that are given in order to describe clearly the reaction process.

3.2 Implications for the delamination model and the destruction of the NCC

The run products, characterized by a lherzolite/pyroxenite/garnet-pyroxenite sequence, have a similar structure as composite mantle xenoliths found by Liu et al. [36], in the Neogene Hannuoba basalt of the NCC. Our experiments support that the mafic lower crust of NCC may have foundered into the asthenosphere in Meso-Cenozoic. Those composite mantle xenoliths should be attributed to the interaction between the melt of foundered eclogite and mantle peridotite.

3.3 Implications for the genesis of high Mg# andesite

At 1300 and 1350°C, melt of eclogite-melt/peridotite reaction possesses a high Mg# andesite signature (Mg#=56), which is very similar to the andesites from Xinglougou Formation and Yixian Formation in western Liaoning, except that the latter have higher K_2O contents [8, 40, 41]. Therefore, the eclogite-melt/peridotite reaction could be responsible for the formation of high Mg# andesite. Previous studies have shown that partial melting of eclogite at high pressure (>3 GPa) will form K-rich melt [37], which indicates that the high Mg# andesites from western Liaoning may be the result of eclogite-melt/peridotite reaction at higher pressure.

4 Conclusions

From the HPHT experimental studies on eclogite-melt/ peridotite reaction we draw the following conclusions:

The products of eclogite-melt/peridotite reaction have the same structure as composite mantle xenoliths from the Hannuoba basalt, which indicate that melts from foundered eclogitised lower crust of the NCC that interacted with mantle peridotite played an important role in the thinning of NCC.

The melts from eclogite-melt/peridotite reaction at 1300 and 1350°C have a high Mg# andesite signature, which indicates that this reaction is a viable mechanism for the genesis of high Mg# andesites.

This work was supported by National Natural Science Foundation of China (Grant Nos. 40802019, 90714005, 40821061), Ministry of Education of China and the State Administration of Foreign Expert Affairs of China (Grant No. B07039) and China Postdoctoral Science Foundation.

1 Fan W M, Zhang H F, Baker J, et al. On and off the North China Craton: Where is the Archean keel? J Petrol, 2000, 41: 933–950
2 Menzies M A, Xu Y G, Zhang H F, et al. Integration of geology, geophysics and geochemistry: A key to understanding the North China Craton. Lithos, 2000, 96: 1–21
3 Niu Y L. Generation and evolution of basaltic magmas: Some basic concepts and a new view on the origin of Mesozoic-Cenozoic basaltic volcanism in Eastern China. Geol J China Univ, 2005, 11: 9–46
4 Zhou X H. Major transformation of subcontinental lithosphere beneath eastern China in the Cenozoic-Mesozoic: Review and prospect (in Chinese). Earth Sci Front, 2006, 13: 50–54
5 Deng J F, Zhao H L, Mo H X, et al. Continental Roots-plume Tectonics of China: Key to the Continental Dynamics (in Chinese). Beijing: Geological Publishing House, 1996
6 Wu F Y, Sun D Y, Zhang G L, et al. Deep geodynamics of Yanshain Movement (in Chinese). Geol J China Univ, 2000, 6: 379–388
7 Gao S, Rudnick R L, Yuan H L, et al. Recycling lower continental rust in the North China Craton. Nature, 2004, 432: 892–897
8 Xu Y G. Roles of thermo mechanic and chemical erosion in continental lithospheric thinning (in Chinese). Bull Miner Petrol Geochem, 1999, 18: 1–5
9 Xu Y G. Thermo-tectonic destruction of the Archean lithospheric keel beneath eastern China: Evidence, timing and mechanism. Phy Chem Earth, 2001 26: 747–757
10 Lu F X, Zheng J P, Li W P, et al. The main evolution pattern of phanerozoic mantle in the Eastern China: The "Mushroom Cloud" model (in Chinese). Earth Sci Front, 2000, 7: 97–107
11 Zhang H F, Zhou X H, Fan W M, et al. Nature, composition, enrichment processes and its mechanism of the Mesozoic lithospheric mantle beneath the southeastern North China Craton (in Chinese). Acta Petrol Sin, 2005, 21: 1271–1280
12 Kay R W, Kay S M. Creation and destruction of lower continental crust. Geol Rund, 1991, 80: 259–278
13 Kay R W, Kay S M. Delamination and delamination magmatism. Tectonophysics, 1993, 219: 177–189
14 Gao S, Jin Z M. Delamination and its geodynamical significance for the crust mantle evolution (in Chinese). Geol Sci Technol Info, 1997, 16: 1–9
15 Yan J, Chen J F, Xie Z, et al. Mantle xenoliths from Late Cretaceous basalt in eastern Shandong Province: New constraint on the timing of lithospheric thinning in eastern China. Chin Sci Bull, 2003, 48: 2139–2144
16 Zhang H F, Nakamura E, Sun M, et al. Transformation of subcontinental lithospheric mantle through peridotite-melt reaction: Evidence from a highly fertile mantle xenolith from the North China Craton. Inter Geol Rev, 2007, 49: 658–679
17 Zhang H F. Transformation of lithospheric mantle through peridotite-melt reaction: A case of Sino-Korean Craton. Earth Planet Sci Lett, 2005, 237: 768–780
18 Zhang H F, Sun M, Zhou M F, et al. Highly heterogeneous Late Mesozoic lithospheric mantle beneath the North China Craton: Evidence from Sr-Nd-Pb isotopic systematics of mafic igneous rocks. Geol Mag, 2004, 141: 55–62
19 Pei F P, Xu W L, Wang Q H, et al. Mesozoic basalt and mineral chemistry of the mantle-derived xenocrysts in Feixian, Western Shandong, China: Constraints on nature of Mesozoic lithospheric mantle (in Chinese). Geol J China Univ, 2004, 10: 88–97
20 Tang Y J, Zhang H F, Ying J F. High-Mg olivine xenocrysts entrained in Cenozoic basalts in central Taihang Mountains: Relicts of old lithospheric mantle (in Chinese). Acta Petrol Sin, 2004, 20: 1243–1252
21 Shao J A, Lu F X, Zhang L Q, et al. Discovery of xenocrysts in basalts of Yixian Formation in west Liaoning Province and its significance (in Chinese). Acta Petrol Sin, 2005, 21: 1547–1558
22 Ying J F, Zhang H F, Kita N, et al. Nature and evolution of Late Cretaceous lithospheric mantle beneath the eastern North China Craton: Constraints from petrology and geochemistry of peridotitic xenoliths from Junan, Shandong Province, China. Earth Planet Sci Lett, 2006, 244: 622–638
23 Zhang H F. Peridotite-melt interaction: An important mechanism for the compositional transformation of lithospheric mantle (in Chinese). Earth Sci Fron, 2006, 13: 65–75
24 Zhang H F, Shao J A. Volcanic lavas of the Yixian Formation in western Liaoning province, China: Products of lower crust delamination or magma mixing (in Chinese)? Acta Petrol Sin, 2008, 24: 37–48
25 Xiong X L, Xia B, Xu J F, et al. Na depletion in modern adakites via melt/rock reaction within the sub-arc mantle. Chem Geol, 2006, 229: 273–292, and reference therein
26 Fisk M R. Basalt-magma interactions with harzburgite and the formation of high magnesium andesites. Geophys Res Lett, 1986, 13: 467–470
27 Kelemen P B, Joyce D M, Webster J D, et al. Reaction between ultramafic rock and fractionating basaltic magma II. Experimental investigation of reaction between olivine tholeiites and harzburgite at 1150–1050ºC and 5 kbar. J Petrol, 1990, 31: 99–134
28 Carroll M, Wyllie P J. Experimental phase relations in the system tonalite-peridotite-H_2O at 15 kbar: Implications for assimilation and differentiation processes near the crust-mantle boundary. J Petrol, 1989, 30: 1351–1382
29 Kelemen P B, Hart S R, Bernstein S. Silica enrichment in the continental upper mantle via melt/rock reaction. Earth Planet Sci Lett, 1998, 164: 387–406
30 Rapp R P, Shimizu N, Norman M D, et al. Reaction between slab-derived melts and peridotite in the mantle wedge: Experimental constraints at 3.8 GPa. Chem Geol, 1999, 160: 335–356
31 Anderson D A. Large igneous provinces, delamination, and fertile mantle. Elements, 2006, 1: 271–275
32 Ravna E K. The garnet-clinopyroxene Fe^{2+}-Mg geothermometer: An updated calibration. J Metamorph Geol, 2000, 18: 211–219
33 Ellis D J, Green D H. An experimental study of the effect of Ca upon the garnet-clinopyroxene Fe-Mg exchange equilibria. Contrib Mineral Petro, 1979, 71: 13–22
34 Pertermann M, Hirschmann M M. Anhydrous partial melting experiments on MORB-like eclogite: Phase relations, phase compositions and mineral-melt partitioning of major elements at 2–3 GPa. J Petrol, 2003, 44: 2173–2201
35 Spandler C, Yaxley G, Green D H, et al. Phase relations and melting of anhydrous K-bearing eclogite from 1200 to 1600ºC and 3 to 5 GPa. J Petrol, 2008, 49: 771–795
36 Liu Y S, Gao S, Lee C A, et al. Melt-peridotite interactions: Links between garnet pyroxenite andhigh-Mg# signature of continental crust. Earth Planet Sci Lett, 2005, 234: 39–57
37 Yaxley G M, Green D H. Reaction between eclogite and peridotite: Mantle refertilisation by subduction of oceanic crust. Schweiz Mineral Petrogr Mitt, 1998, 78: 243–255
38 Morgan Z, Liang Y. An experimental study of the kinetics of lherzolite reactive dissolution with applications to melt channel formation. Contrib Mineral Petrol, 2005, 150: 369–385
39 Kelemen P B. Reaction between ultramafic rock and fractionating basaltic magma I. Phase relations, the origin of calc-alkaline magma series, and the formation of discordant dunite. J Petro, 1990, 31: 51–98
40 Wang X R, Gao S, Liu X M, et al. Geochemistry of high-Mg andesites from the early Cretaceous Yixian Formation, western Liaoning: Implications for lower crustal delamination and Sr/Y variations. Sci China Ser D-Earth Sci, 2006, 49: 904–914
41 Huang H, Gao S, Hu Z C, et al. Geochemistry of the high-Mg andesites at Zhangwu, western Liaoning: Implication for delamination of newly formed lower crust. Sci China Ser D-Earth Sci, 2007, 50: 1773–1786